IEEE Access
Multidisciplinary | Rapid Review | Open Access Journal

Received June 2, 2019, accepted June 26, 2019, date of publication July 8, 2019, date of current version August 6, 2019.

Digital Object Identifier 10.1109/ACCESS.2019.2927321

Ant Colony Optimization PID Control of Hypnosis With Propofol Using Renyi Permutation Entropy as Controlled Variable

ZHENHU LIANG[1], LINGYUN FU[1], XIAOYU LI[1], ZEGUO FENG[2], JAMIE W. SLEIGH[3], AND HAK KEUNG LAM[4]

[1]Institute of Electrical Engineering, Yanshan University, Qinhuangdao 066004, China
[2]Anesthesia and Operation Central, Chinese PLA General Hospital, Beijing 100853, China
[3]Department of Anesthesia, Waikato Hospital, Hamilton 3240, New Zealand
[4]Department of Informatics, King's College London, London WC2B 4BG, U.K.

Corresponding author: Zhenhu Liang (zhl@ysu.edu.cn)

This work was supported in part by the National Natural Science Foundation of China under Grant 61673333 and Grant 61304247, in part by the Natural Science Fund for Excellent Young Scholars of Hebei Province of China under Grant F2018203281, and in part by the Science and Technology Research and Development Program of Qinhuangdao under Grant 201703A153.

ABSTRACT General anesthesia is a critical procedure in clinical surgery. To offer a closed control of depth of hypnosis, we establish a closed-loop anesthetic delivery system for propofol anesthesia. The system consists of three components: 1) three-compartment pharmacokinetic model; 2) a pharmacodynamics model obtained by identifying the relationship of effect–site concentration and Renyi permutation entropy via particle swarm optimization; and 3) ant colony optimization proportion integration differentiation controller. The performance of Renyi permutation entropy and bispectral index in tracking the effect–site concentration is evaluated by the prediction probability. The assessments of the performance of the controller are using: 1) the rising time, percent overshoot, and settling time and 2) median performance error, median absolute performance error, wobble, divergence, and integral absolute error. The results show that the prediction probability of Renyi permutation entropy (0.79±0.13 and mean±standard deviation) is higher than the bispectral index (0.74±0.15). The ant colony optimization proportion integration differentiation controller is quick to respond to sudden changes and maintains the stabilty at the desired depth of hypnosis (rise time and overshoot are 4.53±1.96 min and 3.48±1.49 (%), respectively). In conclusion, the proposed closed-loop anesthetic delivery system has potential value for accurate anesthetic administration.

INDEX TERMS General anesthesia, closed-loop anesthetic delivery system, Renyi permutation entropy, ant colony optimization proportional integral derivative, particle swarm optimization.

I. INTRODUCTION

Establishing a reliable closed-loop anesthetic delivery (CLAD) system is an important issue for anesthetists, engineers, and drug researchers. Currently, drug dose control during surgery depends on anesthetists' experience and the clinical interpretation of patients' physiological information. Surgeries heavily relying on the anesthetists' experience would put patients under the risk of anesthetic overdose or under-dose [1]–[3]. As surgeries usually last for hours, manually maintaining a minute-to-minute close control is difficult. Therefore, we sought to design a stable CLAD system to maintain anesthesia in real time.

The associate editor coordinating the review of this manuscript and approving it for publication was Seyedali Mirjalili.

A. GENERAL ANESTHESIA

General anesthesia (GA) is a drug-induced loss and recovery of consciousness for executing surgical procedures. Anesthesia includes three components: hypnosis (loss of memory), analgesia (pain relief), and muscle relaxation. The sedative anesthetics commonly used in clinic include: 1) inhalation anesthetic agent, such as sevofluorane, isofluorane and devofluorane; 2) intravenous anesthetic agent, such as propofol. Among them, metabolic processes in the body of inhalation anesthetic agents are more complicated than those of

propofol [1]. As an intravenous infusion anesthetic drug, propofol has the merits of: 1) rapidly absorbed and metabolized characteristics, 2) not easy to accumulate in the body, 3) less harmful to the kidneys. Most importantly, the metabolism, mechanism, and effects of anesthesia have been well studied and proven to be stable in different population (age, race, etc.) [4]. Until now, propofol has become an important sedative that is widely used for induction and maintenance in GA. In clinical practices, the administration of anesthesia for inhalation anesthetic agent is more complex than intravenous infusion. A closed-loop inhalation anesthesia system needs to adjust the concentration of the inhalation anesthetic agent as well as the respiratory rate, which is controlled by the anesthesia machine. However, the CLAD system only needs to adjust the speed of the injection pump based on the depth of hypnosis (DoH). The effect of propofol on the central nervous system can be measured by the processed electroencephalogram (EEG) recorded from the frontal brain area. To achieve safe anesthesia, propofol is usually combined with opioids, such as remifentanil, and neuromuscular blocking agents for anesthesia maintenance. Various studies suggested that the intraoperative pain and neuromuscular block cannot be measured by EEG [5]. As proved in [5], hemodynamic measurements can be used in administering opioids during surgery, and the level of neuromuscular blocking can be measured by electromyography. Due to the vast quantities of drugs and their varying effect mechanisms, only propofol is considered in this study.

NOMENCLATURE

TABLE 1. List of abbreviations.

Abbreviation	Meaning	Abbreviation	Meaning
ACO	ant colony optimization	ACO-PID	ant colony optimization Proportional Integral Derivative
BIS	bispectral index	COR	correlation coefficient
CLAD	closed-loop anesthetic delivery	DoH	depth of hypnosis
DRPE	desired Renyi permutation entropy	EEG	electroencephalogram
ERPE	estimated Renyi permutation entropy	ESC	effect-site concentration
GA	general anesthesia	IAE	integral absolute error
PD	pharmacodynamic	PID	Proportional Integral Derivative
P_k	prediction probability	PK	pharmacokinetic
PKPD	pharmacokinetic-pharmacodynamic	PSO	particle swarm optimization
RPE	Renyi permutation entropy	TCI	target controlled infusion

B. THE DOH ASSESSMENT

The DoH index derived from EEG is generally used as the feedback signal in the CLAD system. Many indexes have been proposed as control signals: median frequency [6], spectral entropy [7], bispectral index (BIS) [1], and wavelet-based index [8]. Among these indexes, BIS is the most commonly used for DoH evaluation, and it has been proved to exhibit good performance in both propofol and isoflurane closed-loop controls [9]. As the most widely used depth of anesthesia monitor in the world, BIS can well reflect the state of EEG activity and the changes of awareness and consciousness in patients during operation. It is the de facto gold standard in DoH monitor in clinical practice. Nevertheless, the biggest drawback of BIS is that it is a non-disclosure algorithm, which hinders its clinical application. As an observer in CLAD system, this opaque approach may make the control system unpredictable. Also, Bibian et al. assessed the suitability of using DoH monitors for in closed-loop anesthesia or sedation delivery and demonstrated that the BIS-A2000 and M-entropy algorithm could not obtain an unique linear time-invariant model to capture the dynamic behavioral change in cortical activity [10]. Jin-Oh et al. proposed that the wavelet-based index had a better performance in closed-loop control applications in contrast to BIS [8]. All these studies showed that a reliable DoH index is important in the CLAD system and that the commercially acquired DoH measures do not supply a robust observation for the CLAD.

EEG signals are comprised of macro-scale voltage fluctuations that are a result of ionic currents within millions of neurons in the brain [11]. Numerous studies have proposed that EEG is a non-stationary signal that exhibits chaotic behaviors [12], [13]. Meanwhile, the anesthetic induced hypnosis has a complex effect on the brain, so various nonlinear methods, such as fractal analysis [14], Hurst exponent [15], detrended fluctuation analysis [16], Lyapunov exponent [17], and entropy [18], were utilized for DoH evaluation of the brain.

In all these nonlinear measures, entropy received much attention in recent years [19], [20]. In our previous study, we compared various entropy measures in DoH monitoring [20]. The measures of spectral entropy, wavelet entropy, sample entropy, approximate entropy, Hilbert-huang spectral entropy, fuzzy entropy, Shannon permutation entropy, Renyi permutation entropy (RPE) were analyzed in sevoflurane and isoflurane [20]. The results showed that RPE exhibited better performance in tracking the effects of anesthetics on EEG. These findings lead us to determine whether employing the RPE measure as the observation in the CLAD system is possible [20].

So, in this study, we use the RPE as the observation and compared the performance of RPE with the BIS index, which is widely used in DoH monitoring, for propofol anesthesia. The prediction probability (P_k) is employed as an indicator for performance assessment in tracking the effect-site concentration (ESC) of propofol [21].

C. THE VIRTUAL PATIENT MODEL

To accomplish the closed-loop anesthesia control simulation, a virtual patient model library was established and used to analyze the closed-loop anesthetic control. The pharmacokinetic–pharmacodynamic (PKPD) model is a mathematical tool for predicting the effect and efficacy of drug dosing over time. There are some commonly used PKPD

models, such as Marsh's model [22], Schnider's model [23], and Schuttler's model [24]. However, no model has been regarded as gold standard model for the target controlled infusion (TCI) system yet. Until now, Schnider's and Marsh's models have been widely applied in the TCI system [4]. Compared with Marsh's model, Schnider's model, which considers more of the patients' personal information, is relatively more appropriate for personalized TCI. Besides, the experimental study showed that Schnider's model needs less propofol when it is applied in TCI [25]. Therefore, the three-compartment PKPD model proposed by Schnider was chosen to establish the virtual patient model in our study.

The pharmacodynamics (PD) model describes the relationship between drug concentration and the effects on central nervous system. This relationship is nonlinear and the corresponding parameters in PD model are unknown. Thus, we need to select the appropriate identification algorithm to identify the parameters of PD model. The particle swarm optimization (PSO) algorithm can be regarded as a kind of intelligent search algorithm. It is an evolutionary computation method, which has been successfully applied in optimization problems in science and engineering involving nonlinear functions [26]. In this study, we identified the relationship between ESC and RPE with PSO algorithms for comparison.

D. THE CHOICE OF CONTROL ALGORITHM

In the aspect of control methods used in the CLAD, several researchers developed modern control approaches to anesthesia control simulation [27]. The results yielded better tracking performance than manual control, but these approaches still did not achieve good performance in response time and were unable to guarantee stability. Proportional Integral Derivative (PID) controller is a widely used industrial control method with the advantages of a simple principle, in the meantime, only few parameters are tuned when PID controller is used. Besides, its behavior is well understood and intuitive. Some existing studies have shown that PID controller can be used for the study of anesthesia closed-loop control [1], [2]. Also, as proved in [28], a robust PID was introduced to control the propofol anesthesia for children. Different PID parameters were set based on age and body weight. Ant colony optimization (ACO) is an efficient parallel search algorithm. Moreover, it is adaptive and easy to combine with other algorithms. To automatically optimize the parameters of PID controller, we sought to use ACO to optimize the parameters of PID controller. In the meantime, previous studies showed that the PID controller optimized by ACO has excellent performance in direct current motor control [29] and automatic voltage regulation [30]. Especially, in [31], the ant colony optimization Proportional Integral Derivative (ACO-PID) was proposed for controlling of artificial hearts. It indicated that the ACO-PID has satisfactory performances and has good robustness. Therefore, in this study, the ACO-PID controller was employed to perform the CLAD system, in which the ACO is used to change the proportional, integral, and derivative parameters of the PID controller control algorithm.

In this study, we established a closed-loop anesthesia control system for personalized propofol anesthesia. RPE was first proposed to be as a DoH index for the CLAD system's estimator. Using ACO-PID controller, the simulation showed that the control system had the characteristics of minor error, small fluctuation and high stability. The information of the virtual patient model were obtained from the actual patient's clinical administration. At the same time, the actual drug delivery rate in clinical practice was used for simulation. These settings make the simulation process closer to the actual clinical practice. Therefore, the proposed closed-loop anesthesia control system has a potential application value in clinic.

However, it is unrealistic and risky to do clinical tests when the method and control system have not been evaluated with simulation and off-line analysis. Thus, the purpose of this study is to evaluate the method and performance of system with off-line simulation before further clinical testing and guidance.

This paper is organized as follows: In Section 2, observation and definition of the RPE, PKPD model, controllability and observability of system, the methods used in identification part, the controller module, and statistical analysis are presented. In Section 3, the evaluation of RPE performance, identification of PD model and CLAD system simulation are presented. In Section 4, we discuss the present work results and give directions in future research. Lastly, the conclusion is given in Section 5.

II. THEORY

The CLAD system includes the control signal (①), the PKPD model (② and ③), the identification module (④), and the controller (⑤). The block diagram of the CLAD system is exhibited in Fig. 1.

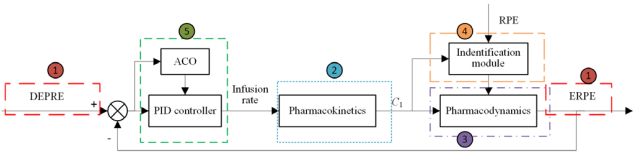

FIGURE 1. Block diagram of the CLAD system.

The procedures of the control system can be described as follows: Firstly, we calculated the RPE value, which was obtained by analyzing the actual clinical EEG data collected from the clinic during propofol anesthesia. Next is the PKPD model, which includes two models, the pharmacokinetic (PK) model (②) and the PD model (③). The input of the PK model was the clinical drug injection rate (mg/kg/h), which was used to calculate the corresponding central compartment drug concentration. The input of PD model was the central compartment drug concentration, and then, the ESC was calculated. Then, the identification module (④) used PSO

for parameter identification, the real RPE values and relevant ESC values were used as the inputs of PSO and then combined with PD model, the estimated RPE is obtained. In order to distinguish the RPE obtained by EEG recordings from the output of the PD model, the estimated RPE by the PD model is defined as ERPE. The reference input is the desired RPE, which is defined as DRPE. Finally, the ACO-PID controller (⑤) calculated the infusion rate of the anesthetic, the input of which was the error between the ERPE value obtained by PD model and the DRPE value.

A. OBSERVATION AND DEFINITION OF THE RPE

The RPE is a complexity measure for a time series based on the nonlinear ordinal analysis and Renyi entropy [20]. Renyi entropy is a generalized entropy that can provide additional information about specific events compared with the Shannon entropy. The details of the RPE measure are described as follows:

Given a time series $x(t)$, $(1 \leq t \leq N)$, which represents the EEG signals collected from forehead in this study. The time series $x(t)$ was mapped into a m dimensional space, with τ as the time delay, which can be expressed by vectors X_t and be defined as follows:

$$X_t = [x(t), x(t+\tau), \ldots, x(t+(m-1)\tau)] \tag{1}$$

where X_t is an m equally-spaced samples vector from $x(t)$. For any given number t, rearrange X_t in an increasing order, which is defined as follows:

$$[x\,(t+(j_1-1)\,\tau \leq x\,(t+(j_2-1)\,\tau \cdots \leq x\,(t+(j_m-1)\,\tau)] \tag{2}$$

For m different numbers, there will be $m!$ possible permutations [32]. Thus, every vector X_t in the m dimensional space can be mapped by one of the $m!$ possible permutations. Each permutation is treated as a symbol, so this reconstruction sequence can be seen as a sequence of symbol. The probability of j_{th} permutation mode occurring is defined as P_j, which can be calculated as follows:

$$p_j = \frac{n_j}{\sum_{j=1}^{m!} n_j} \tag{3}$$

where j represents permutation mode, and n_j is the number of vectors in each permutation mode. Then RPE can be defined as follows:

$$\mathrm{RPE} = \frac{\log \sum_{j=1}^{m!} p_j^a}{(1-a) * \ln(m!)} \tag{4}$$

where a is the selector of probability, which can tune the sensitivity of RPE in measuring the randomness of EEG signal. According to the references [19], [26], we choose $m = 6$, $\tau = 1$ and $a = 2$ for the RPE calculation. To achieve a consistent index range with the ERPE derived from the PKPD, the index range of the RPE, which ranges from 0 to 1, is expanded to [0 100].

B. PKPD MODEL

The PKPD model is important for describing the drug metabolism and predicting the effect and efficacy of drug dosing over time. It consists of two parts: PK and PD models. The PK model describes the concentration of drugs in tissues over time, and the PD model describes the drug effects on the body by linking the plasma concentration to an efficacy metric. The Schnider propofol model has been verified to be suitable to the TCI system [4], in this study, we built the virtual patient models based on the Schnider propofol model. The block diagram of PKPD model is shown in Fig. 2.

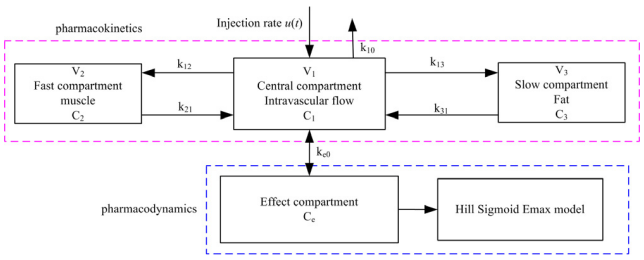

FIGURE 2. Three-compartment PKPD model block diagram.

The PK model is modeled by a third-order differential equation, which is established based on mass balance theory and described as follows, and the details of the parameters are presented in [1], [4].

$$\begin{cases} \frac{\mathrm{d}C_1(t)}{\mathrm{d}t} = -(k_{10}+k_{12}+k_{13})C_1(t) + k_{21}\frac{V_2}{V_1}C_2(t) \\ \qquad\qquad +k_{31}\frac{V_3}{V_1}C_3(t) + \frac{1}{V_1}u(t) \\ \frac{\mathrm{d}C_2(t)}{\mathrm{d}t} = k_{12}\frac{V_1}{V_2}C_1(t) - k_{21}C_2(t) \\ \frac{\mathrm{d}C_3(t)}{\mathrm{d}t} = k_{13}\frac{V_1}{V_3}C_1(t) - k_{31}C_3(t) \end{cases} \tag{5}$$

In these equations, C_1 represents the drug concentration in the central compartment [μg/ml], while C_2 and C_3 represent the drug concentration in the fast compartments and in the slow equilibrating peripheral compartments, respectively. The central compartment refers to intravascular blood. The fast compartment is defined as the tissues of the rapid distribution, such as muscle. And the slow compartment is defined as the tissues of the slow distribution, such as fat. The $u(t)$ is the input of PK model and whose unit is [mg/kg/h]. The parameter k_{10} is the eliminating rate of anesthetic. The parameter $k_{ij}(i, j = 1, 2, 3, i \neq j)$ denotes the drug transfer coefficient from the i_{th} to j_{th} compartment, and they depend on the patients' weight, height, age, gender and so on [1], [2].

$$k_{10} = \frac{C_{l1}}{V_1}, k_{12} = \frac{C_{l2}}{V_1}, k_{13} = \frac{C_{l3}}{V_1}, k_{21} = \frac{C_{l2}}{V_2}, k_{31} = \frac{C_{l3}}{V_3} \tag{6}$$

where C_{l1},C_{l2} and C_{l3} represent the clearance rates of the relevant compartments. Where V_1, V_2 and V_3 represent the volume of central compartments, the volume of fast compartments, the volume of slow compartments,

respectively.

$$V_1 = 4.27,\ V_2 = 18.9 - 0.391 \times (age - 53),\ V_3 = 238 \tag{7}$$

$$C_{l1} = 1.89 + 0.0456 \times (weight - 77) - 0.0681 \times (lbm - 59) + 0.0264 \times (height - 177) \tag{8}$$

$$C_{l2} = 1.29 - 0.024 \times (age - 53) \tag{9}$$

$$C_{l3} = 0.836 \tag{10}$$

$$lbm = \begin{cases} 1.07 \cdot weight - 148 \cdot \dfrac{weight^2}{height^2}, & \text{female} \\ 1.1 \cdot weight - 128 \cdot \dfrac{weight^2}{height^2}, & male \end{cases} \tag{11}$$

where *lbm* is lean body mass.

Based on the formulas (6) - (11) and actual patients' physiological information, we can get each range of the drug transfer coefficient k_{ij} and showed in Table 2.

TABLE 2. Drug transfer coefficient between different compartments.

Coeffici ent	k_{10}	k_{12}	k_{21}	k_{13}	k_{31}	k_{e0}
Range	0.337 - 0.476	0.848 - 1.872	0.097 - 0.456	0.285 - 0.567	0.008 - 0.070	0.025 - 5.000

The PD model consists of a first-order differential equation and a nonlinear Hill equation, which is designated to combine the drug concentration with DoH index. The PD model is as follows:

$$\frac{dC_{\text{eff}}(t)}{dt} = k_{e0}(C_1(t) - C_{eff}(t)) \tag{12}$$

$$ERPE(t) = E_{\max} - (E_{\max} - E_{\min}) \cdot \frac{C_{eff}(t)^{\gamma}}{EC_{50}^{\gamma} + C_{eff}(t)^{\gamma}} \tag{13}$$

where C_{eff} and C_1 represent the drug concentration in the effect-site compartment and in the central compartment, respectively. The parameter k_{e0} is the transfer ratio between the effect-site compartment and the central compartment. C_{eff} can be calculated by equations (5) to (12), which is a vector as the input of equation (13).

For equation (13), $E_{\max}$ and $E_{\min}$ represent the maximum and minimum ERPE, respectively, EC_{50} is the drug concentration at which the ERPE is at half maximum, and γ is the slope of the Hill equation curve. The four parameters $E_{\max}$, $E_{\min}$, EC_{50}, and γ are the parameters of individual patient to be determined and they might change during the process of anesthesia triggered by surgical stimulation or drug interaction.

The incorporation of the three-compartment PK model and the identified PD model constructs the virtual patients for simulation.

1) PERFORMANCE OF THE SYSTEM

By transforming equation (5) into the state equation, PK model can be represented by equation (14).

$$\begin{aligned} \frac{dC(t)}{dt} &= \mathrm{A} \cdot C(t) + \mathrm{B} \cdot u(t) \\ C_{pk} &= \mathrm{D} \cdot C(t) \end{aligned} \tag{14}$$

where C_{pk} is the output of PK model.

$$\mathrm{A} = \begin{bmatrix} -(k_{10} + k_{12} + k_{13}) & \dfrac{V_2}{V_1}k_{21} & \dfrac{V_3}{V_1}k_{31} \\ \dfrac{V_1}{V_2}k_{12} & -k_{21} & 0 \\ \dfrac{V_1}{V_3}k_{13} & 0 & -k_{31} \end{bmatrix} \tag{15}$$

$$\mathrm{B} = \begin{bmatrix} \frac{1}{V_1} & 0 & 0 \end{bmatrix} \tag{16}$$

$$\mathrm{D} = [\,1\ 0\ 0\,] \tag{17}$$

As we know, the relationship between state space expression and transfer function is as follows:

$$\mathrm{W}(s) = \mathrm{D}(sI - \mathrm{A})^{-1}\mathrm{B} \tag{18}$$

According to the above relationship, we can convert the equations of (15) - (17) into equation (19), as shown at the bottom of this page.

So the characteristic expression is shown in equation (20).

$$s^3 + (k_{10} + k_{12} + k_{13} + k_{21} + k_{31})s^2 + (k_{10}k_{21} + k_{10}k_{31} + k_{12}k_{31} + k_{13}k_{21} + k_{21}k_{31})s + k_{10}k_{21}k_{31} = 0 \tag{20}$$

Because all coefficients of the characteristic equation are positive, and

$$(k_{10} + k_{12} + k_{13} + k_{21} + k_{31})(k_{10}k_{21} + k_{10}k_{31} + k_{12}k_{31} + k_{13}k_{21} + k_{21}k_{31}) > k_{10}k_{21}k_{31} \tag{21}$$

According to Routh criterion, the model is stable. Also, according to equation (19), as long as the k_{12} and k_{13} are not zero (actually they are not), there is no zero-pole cancellation between the denominator and the molecule in the transfer function. Therefore, the system is controllable and observable.

C. STATE MODEL IDENTIFICATION

The PD model parameters were identified by using the PSO based on propofol anesthesia EEG data set.

1) THE SPECIFIC IDENTIFICATION PROCESS OF PSO

PSO is a stochastic optimization technique inspired by bird flocking or fish schooling. Compared with other evolutionary computation algorithms, such as genetic algorithms [33]–[36], the PSO has no evolution operators [37]. Detailed description of PSO can be found in the Appendix B.

$$W(s) = \frac{1}{V_1} \frac{(s + k_{21})(s + k_{31})}{s^3 + (k_{10} + k_{12} + k_{13} + k_{21} + k_{31})s^2 + (k_{10}k_{21} + k_{10}k_{31} + k_{12}k_{31} + k_{13}k_{21} + k_{21}k_{31})s + k_{10}k_{21}k_{31}} \tag{19}$$

Finally, the parameters of PSO were set with the following parameters: group size $N = 80$, maximum velocity of particles $V_{\max} = 1$, and maximum position of particles $Y_{\max} = 100$.

2) THE EVALUATION OF IDENTIFICATION RESULTS

In order to assess the identification results, the fitness is used, which is defined as follows:

$$fitness = \left(1 - \frac{\|r - \hat{r}\|}{\|r - \bar{r}\|}\right) \cdot 100\% \tag{22}$$

where r is the RPE index value calculated from the EEG recordings, $\hat{r}$ is the ERPE index obtained by the identification method, and $\bar{r}$ is the average value of r. A high fitness value means that the model and the actual value have small difference with each other.

D. THE EEG RECORDING AND PREPROCESSING

To identify the model parameters of PD to achieve an accurate ERPE estimation in the control system, we examined two EEG data sets from twelve subjects. The first data set had eight human volunteers introduced in a previous study [38], who were only injected with propofol during the procedure. The second EEG data set included 8 patients undergoing outpatient elective colonoscopy procedure in the Anesthesia and Operation Center, Chinese PLA general hospital. Detailed information on the data set can be found in the Appendix C.

Several procedures were adapted to reduce artifacts before DoH index extraction. First, the raw EEG amplitude values larger than 200 μV which were considered as noise was removed. Second, a classical adaptive noise canceling was employed to reduce the 50 Hz power line interference. The least-mean-square adaptive algorithm was utilized to adjust the filter. Third, a zero-phase digital filter (*filtfilt.m*, butterworth order = 3) was used to obtain the EEG recording in the frequency band of 0.1 - 45 Hz. Finally, the EEG recording was resampled to 100 Hz for RPE calculation. The EEG recordings which had a noisy data length of more than 20% were not considered for analysis. Finally, 12 subjects were enrolled for PD model parameters identification.

E. CONTROLLER DESIGN

In this study, we use the ACO-PID control method as the CLAD system controller. The PID controller algorithm is widely used in industrial control systems for its simple structure. It calculates the error between the desired and the measured value. It is mainly made up of three separate parameters, namely, proportional K_p, integral K_i, and derivative K_d. The differential equation of this control algorithm is expressed as follows:

$$d(t) = K_p e(t) + \frac{1}{T_i}\int_0^i e(t)dt + T_d\frac{de(t)}{dt} \tag{23}$$

where K_p is proportional coefficient, T_i is the integral constant, and T_d is the differential constant, respectively, $e(t)$ is the error between the actual ERPE and the DRPE, and $d(t)$ is the output of the controller.

Traditional PID controller parameters' adjustment method cannot guarantee the most optimum results. Therefore, the optimization algorithm ACO is developed for auto-tune PID controller to improve the control performance. The process of ACO tuning PID controller parameters is depicted in Fig. S1. The specific optimization process of ACO can be seen in the Appendix D.

To select a suitable iteration, we test the number from 40 to 400 with an interval of 20. The results showed that the 40 - 60 iterations can find a similar optimal solution for identification as simulated in 400 iterations. The computation cost will greatly increase if the number of iterations is set too large. To achieve a reliable and relatively fast identification, we chose 60 as the iteration number.

F. STATISTICAL ANALYSIS

In this study, to compare the performance of BIS and RPE in tracking the ESC of propofol, we calculated P_k [21]. The P_k was defined as:

$$P_k = \frac{P_c + P_{tx}/2}{P_c + P_d + P_{tx}} \tag{24}$$

where P_c is the random probability of two data points,P_{tx} is the independent probability of two data points, and P_d is an alternative consistent or inconsistent probability. $P_k = 1$ of the RPE or BIS meant that the indices could correctly predict the ESC of propofol. A P_k value of 0.5 indicated that indicators (RPE or BIS) were no better than chance in predicting the ESC of propofol. Considering the decrease of RPE and BIS with the increase of propofol concentration, the P_k value was replaced by $1 - P_k$ in this study. Detailed information on P_k can be found in the Appendix E.

In order to compare the correlation between BIS and RPE, we calculated the correlation coefficient (COR).

The correlation coefficient is a measure of the degree of linear correlation between two variables $x(t)$ and $y(t)$. Its formula is as follows:

$$\mathrm{COR}(t) = \frac{\mathrm{cov}(x(t),y(t))}{\sqrt{\mathrm{var}(x(t))\mathrm{var}(y(t))}} \tag{25}$$

where, $\mathrm{cov}(x(t),y(t))$ is the covariance of $x(t)$ and $y(t)$. The $\mathrm{var}(x(t))$ and $\mathrm{var}(y(t))$ are the variance of $x(t)$ and $y(t)$, respectively. The correlation coefficient describes the degree of correlation between $x(t)$ and $y(t)$. The range of values for $\mathrm{COR}(t)$ is [-1, 1]. If $\mathrm{COR}(t) > 0$, there is a positive correlation between $x(t)$ and $y(t)$. Whereas, there is a negative correlation between $x(t)$ and $y(t)$ when $\mathrm{COR}(t) < 0$. In this study, we used the absolute value of COR, i.e., $|\mathrm{COR}(t)|$, to measure the correlation degree of two index. The $|\mathrm{COR}(t)|$ value greater than 0.8 is high correlation, between 0.5 and 0.8 is medium correlated, between 0.3 and 0.5 is low correlated, and less than 0.3 indicates no correlation [39].

The performance of target tracking in the control system is explained by rise time, overshoot, and settling time. Rise time is defined as the time from the start of the change point to the

point at which the ERPE first reaches the target, and settling time is defined as the time span of the controller needed from onset to the time point of the controller stabilizing within 5% of the target. Overshoot is the percent difference between the steady value and the target measure. These metrics are calculated for the target ERPE tracking in three phases: I. Induction stage (0 min $<$ t $<$ 10 min), II. deep anesthesia stage (10 min $<$ t $<$ 30 min), and III. shallow anesthesia stage (30 min $<$ t $<$ 50 min).

Furthermore, some statistical metrics, which are widely used in closed-loop anesthesia system [40], including median performance error (*MDPE*), median absolute performance error (*MDAPE*), *wobble*, and *divergence*, are calculated based on error for CLAD performance evaluation. The details (26)–(30), as shown at the bottom of this page.

The meanings of these metrics are described as follows: 1) The symbol of *error* in equation (26) is defined as the error between the ERPE obtained by system and the DRPE. 2) *MDPE* is a measure of bias, whose meaning is the median error. It is a signed value and can reflect the overdose or under-dose of anesthetics. When *MDPE* is positive, it indicates that the anesthetic drug is under-dose, otherwise, the anesthetic drug is overdose. 3) *MDAPE* can reflect the inaccuracy of the control system. 4) *Wobble* can measure the variability of the performance error. 5) *Divergence* is often used to assess the expected systematic time-related changes of performance. If *divergence* is a positive value, it means the output of system diverges from the DRPE, otherwise, it means that the output of system converges to the DRPE [40].

In addition, the performance of rejecting disturbance is evaluated by integral absolute error (IAE), which is defined as follows:

$$\mathrm{IAE} = \int_0^t |e(t)dt| \tag{31}$$

where $e(t)$ is the errors between the DRPE and ERPE. A smaller of the IAE value means the better anti-jamming performance of the system.

III. RESULTS

A. THE EVALUATION OF RPE PERFORMANCE

Fig. 3. shows a patient's EEG recording during propofol anesthesia, corresponding ESC estimated by PKPD model, BIS value collected from BIS monitor and RPE calculated from EEG. It can be seen that the BIS and PRE have similar trend during propofol anesthesia.

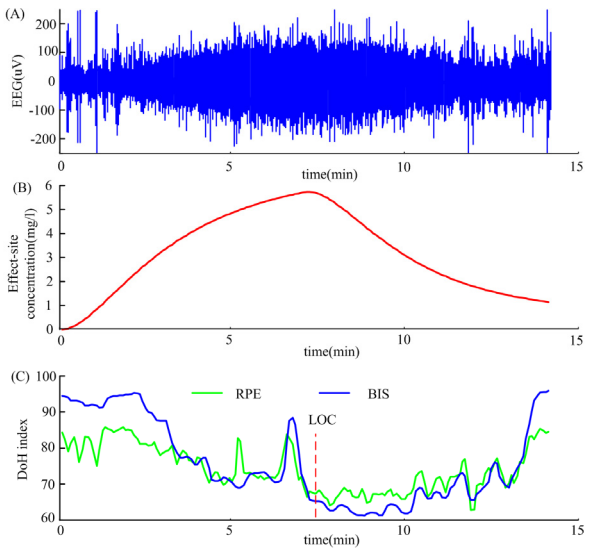

FIGURE 3. EEG recording and corresponding indicators. (A) EEG signal of a patient. (B) ESC calculated by PKPD model. (C) RPE calculated by EEG signal and BIS collected by BIS monitor.

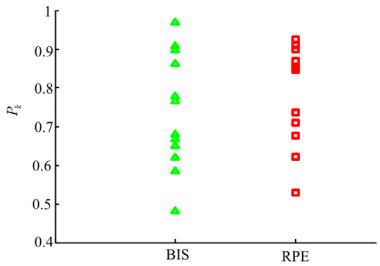

FIGURE 4. The P_k of RPE and BIS for 12 patients.

In order to evaluate the performance of RPE in tracking the ESC of propofol, we compared the P_k value of both RPE and BIS. The P_k values of 12 patients' RPE and BIS indices are represented in Fig. 4. Both the BIS and RPE have high P_k values. The statistics showed that RPE has a higher predictive performance (0.79±0.13, mean ± standard deviation (mean ± SD)) than BIS (0.74±0.15).

In addition, we calculated the correlation coefficient (COR) between RPE and BIS. The statistics of the COR

$$error = \frac{ERPE - DRPE}{DRPE} \tag{26}$$

$$MDPE = median\,(error) \tag{27}$$

$$MDAPE = median(abs(error)) \tag{28}$$

$$Wobble = median\,\{|error - median\,(error)|\} \tag{29}$$

$$divergence_i = 60 \times \frac{\sum_{j=1}^{N_i} \left|error_{ij}\right| \times t_{ij} - (\sum_{j=1}^{N_i} \left|error_{ij}\right|) \times (\sum_{j=1}^{N_i} t_{ij})/N_i}{\sum_{j=1}^{N_i} (t_{ij})^2 - (\sum_{j=1}^{N_i} t_{ij})^2/N_i} \tag{30}$$

TABLE 3. The COR of RPE and BIS for all patients.

Patient	COR	Patient	COR	Patient	COR
1	0.87	5	0.95	9	0.62
2	0.88	6	0.69	10	0.61
3	0.92	7	0.76	11	0.65
4	0.62	8	0.77	12	0.75

are shown in Table 3. It can be seen that the all the COR values are higher than 0.6, which demonstrates that RPE and BIS have a high and medium correlation and index range during anesthesia. So, similar to the BIS, we set the index range of RPE with moderate anesthesia as 40 - 60 for CLAD simulation.

B. IDENTIFICATION OF THE PD MODEL

By taking the propofol infusion velocity and drug stop time, which are described in [38], as the inputs of the PKPD model, we obtain the ESC of each patient. Fig. 5. illustrates the relationship between the ESC and the RPE obtained by analyzing the recorded EEG of twelve patients. All sections feature a clockwise hysteresis loop, which reflects the lag between two variables. Fig. 5. also verifies that no strict one-to-one relationship exists between two variables. Compared with the ESC increasing phase, the same concentration corresponds to a small RPE in the decreasing phase.

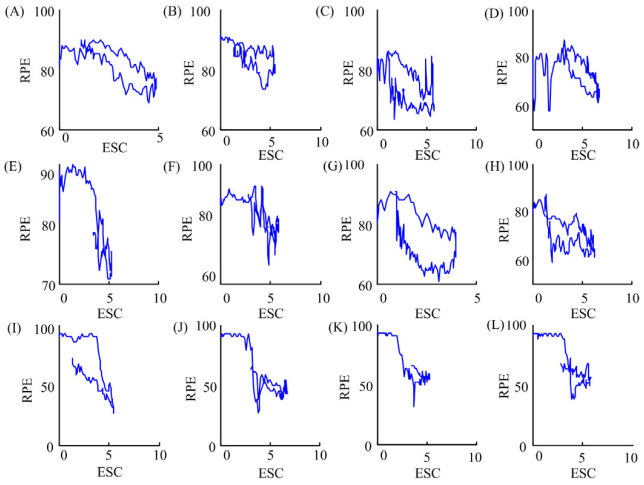

FIGURE 5. Plots of RPE obtained by EEG versus effect-site concentration ($\mu g/ml$)).

In this study, we used PSO to identify the PD model parameters. After 20 simulation trials, the best results by using PSO are chosen and shown in Fig. 6. The fitness statistics results of PSO are shown in Table 4.

The identification results with the degree of fitness more than 50% are considered for virtual patients' construction. In our experiments, we found that when the fitness value is less than 50%, the identified PD model was inconsistent with

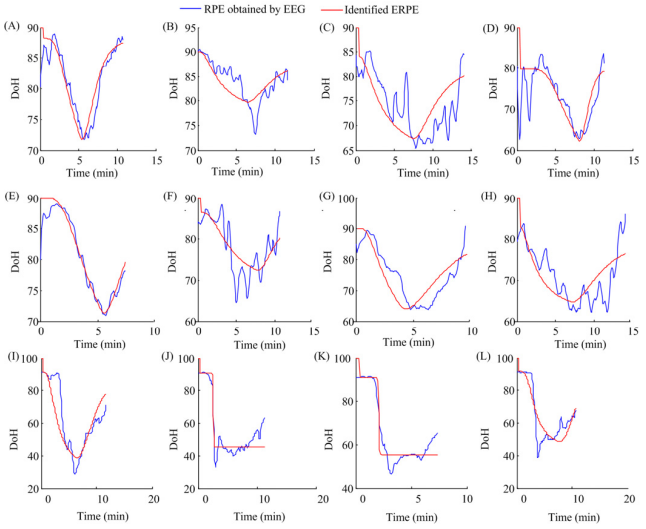

FIGURE 6. Plots of RPE obtained by EEG data (blue line) and identified ERPE (red line) by PSO algorithm. (1–12) represent the patient number.

TABLE 4. The fitness of the PSO for 12 patients (1 to 12) (%).

Patient	fitness	Patient	fitness	Patient	fitness
1	73.9	5	78.6	9	57.6
2	**45.1**	6	62.8	10	84.3
3	**30.4**	7	56.7	11	86.6
4	68.9	8	**43.9**	12	85.7

the actual situation of the patient. Under these conditions, the model does not represent the actual patient situation very well. In order to achieve a balanced sample of virtual patients with real subjects enrolled, the PD parameters of patients 2, 3, and 8, whose fitness values are less than 50% (see in Table 4), were reconstructed based on the average of those patients with the fitness more than 50% [41]. The 2, 3, and 8 patient's PD model parameters are obtained by taking the average of the parameters of 4 and 5, 4 and 6, 5 and 6, respectively. The identification parameters of 12 virtual patients obtained by PSO are showed in the Table 5.

C. THE CLAD SYSTEM SIMULATION

Before the simulation, we need to design DRPE curves. Traditional classification for anesthesia is Guedel's classification. Guedel's classification for anesthesia is mainly aimed at a sole inhalational anesthetic agent, whose classification depend upon the muscular movements [42]. Guedel divides anesthesia into four phases: analgesia, excitement, surgical anesthesia, respiratory paralysis [43]. However, for the closed-loop control of anesthesia, most of the researchers divided the anesthesia procedure into three phases: induction, maintenance and emergence [8], [44]. Furthermore, the process of closed-loop control anesthesia does not need to consider the recovery phase for the drug had ceased in this phase.

TABLE 5. Biometric values of the 12 patients obtained by identification of PSO.

Patient	Age	Weight[kg]	Height[cm]	gender	E_{max}	E_{min}	γ	EC_{50}
1	39	98	191	M	88.2	21.9	2.44	7.70
2	26	78	179	M	84.7	10.5	3.55	10.5
3	30	120	198	M	83.2	25.7	3.57	9.64
4	26	81	178	F	79.8	21.1	5.50	7.91
5	37	78	177	M	89.4	0.00	1.60	13.1
6	27	95	183	M	86.5	30.3	1.63	11.4
7	42	68	165	F	90.1	0.00	1.05	9.46
8	36	89	176	M	88.0	15.1	1.61	12.2
9	41	66	169	F	91.5	5.72	1.70	4.14
10	40	65	165	F	93.1	27.7	2.87	20.9
11	43	57	165	M	91.2	55.4	1.82	40.9
12	39	73	169	M	93.2	2.86	1.26	4.04

TABLE 6. Optimized PID parameters by ACO.

Patient	K_p	K_i	K_d	Patient	K_p	K_i	K_d
1	30	0.47	10.8	7	30	0.41	12.9
2	30	0.29	9.62	8	27.8	0.41	15.8
3	30	0.30	10.0	9	30	0.28	14.3
4	30	0.29	8.50	10	30	0.22	12.7
5	30	0.20	14.3	11	30	0.23	11.9
6	30	0.23	9.67	12	27.4	0.35	13.0

Considering the real procedures during surgery, we divided anesthesia into three phases: induction, deep anesthesia, and shallow anesthesia according to clinical monitoring devices such as the BIS monitor, in which the deep anesthesia and shallow anesthesia are included in the maintenance phase. The ERPE set points of three phases (induction, deep anesthesia and shallow anesthesia) are 70, 40, and 60, respectively. The closed-loop control of propofol is simulated using the ACO-PID algorithm. For the ACO control, the numbers of population, variables, and iterations are 40, 3, and 60, respectively. The PID controller parameters optimized by the ACO are summarized in Table 6. Notably, the manipulated variable u, that is, the propofol infusion rate, is usually limited to 0 - 40 mg/kg/h to ensure the patients' safety [45].

Fig. 7. shows the results of the propofol auto control. Fig. 7.(A) illustrates the DRPE and ERPE obtained by PD model of twelve patients. Clearly, the ERPE obtained by PD model can track the target curves precisely by reacting to the desired changes rapidly and maintaining the desired value. Fig. 7.(B) illustrates the manipulated propofol infusion rate adjusted by the controller. Different colors represent different patients. Among all the patients, patient 12 is the most sensitive one, with a large ERPE decrease and a small

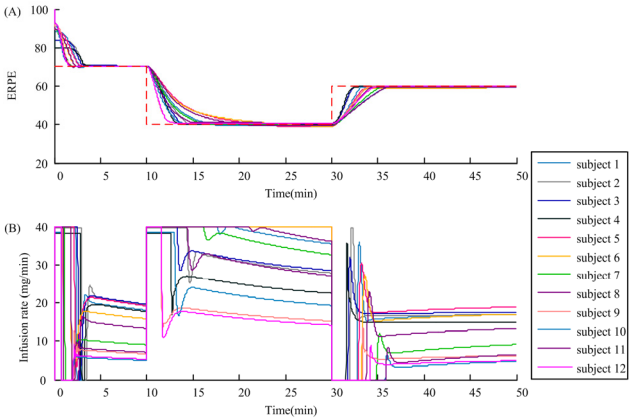

FIGURE 7. (A) Closed-loop response of ERPE (solid line) and the target curve (dotted line). (B) Propofol infusion rate of twelve patients. Different color represents different subjects.

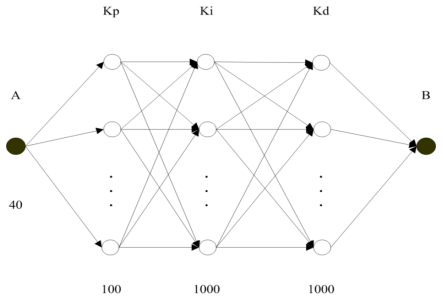

FIGURE 8. Diagram of ACO tuning PID parameters. The parameters K_p, K_i and K_d are designed as nodes. Each path of ant colony contains three nodes which come from the three parameters. Ants constantly release pheromones when they move. When other ants choose the path, if they find the path with pheromone, they tend to choose to move along the path, which strengthens the pheromone concentration of the path. However, with the passage of time, pheromones on the path will continue to volatilize, and the attraction to ants will decrease. Compared with longer paths, ants spend less time passing through shorter paths, and pheromone concentration in shorter paths is often higher than that in longer paths. Ultimately, the whole ant can find the best path. They can be considered as probabilistic multi-agent algorithms using a probability distribution to make the transition between each iteration [64].

amount of propofol. While, patient 6 is considered as an insensitive patient. When these patients' DoH indices are the same, patient 6 needs more anesthetic drug. In order to better illustrate the system's robustness, we divided the maintenance phase into four stages and set another target curve at 50, 40, 60, and 50. Each of these stages lasted 10 minutes except the last stage which lasted for 20 minutes. In this condition, the target curve represents a more complex surgical procedure, and simulation results are shown in Fig. 9. The results show that the ERPE obtained by PD model can track the target curves precisely by reacting to the desired changes rapidly and consistently maintaining the desired value. In addition, we added the artificial noises to test the performance of rejecting disturbance, the standard stimulus profile is shown in Fig. 10 [41]. In this profile, each interval represents a specific stimulus disturbance during the surgery. The simulation results are shown in the Fig. 11.

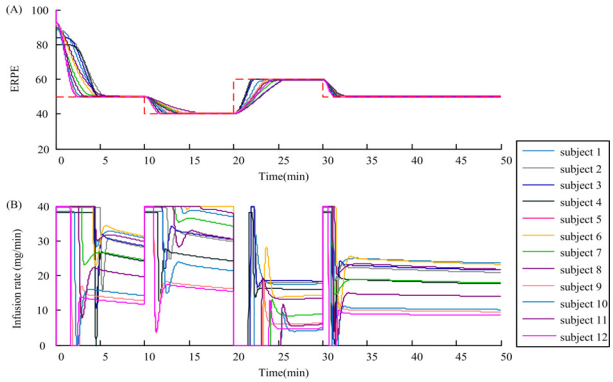

FIGURE 9. (A) Closed-loop response of ERPE (solid line) and the target curve (dotted line). (B) Propofol infusion rate of twelve patients. Different color represents different subjects.

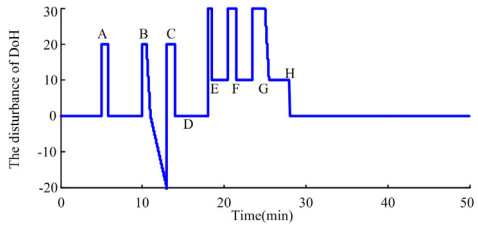

FIGURE 10. The simulated disturbance signal.

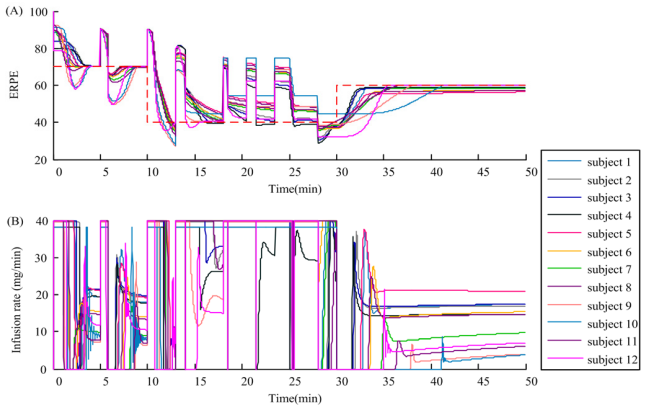

FIGURE 11. The simulation of the 12 patients with surgery stimulation. (A) Closed-loop response of ERPE with artificial disturbance (solid line) and the target curve (dotted line). (B) Propofol infusion rate of twelve patients. Different color represents different subjects.

To evaluate the control performance, we adopted two sets of assessment indicators. The first set of evaluations assessing the tracking ability of the simulations is summarized in Table 7, whose form is mean ± SD. Compared with the references of [44], [46], the overshoot of the three phases is smaller, thus indicating a good stationarity of the system, and the rise time and settling time are also smaller, which reflects the rapid response of the system, which are also within the tolerance.

Another performance assessment of the closed-loop anesthesia control system is evaluated by the indices of *MDPE*, *MDAPE*, *wobble*, and *divergence*. The evaluation results are shown in Table 8. The mean of *MDPE*'s absolute values and mean of *MDAPE* values are small, which indicate that the system has relative precisely control performance. The mean value of *wobble* of all the patients is small, which indicates small overall oscillations in the simulation. The mean value of *divergence* of 12 patients is a negative value, which reflects that the ERPE obtained by PD model converges to the DRPE. It also can be seen that the IAE values are less than those in the reference of [47], which employ the similar infusion profiles with our study. Also, the ACO-PID controller can rapidly react to desired changes with a small overshoot. It can also precisely maintain the desired DoH, which is essential in clinical practice. Altogether, the metrics suggest that the ACO-PID is simple and may be able to meet the stringent performance requirements of anesthesiologists.

TABLE 7. Setpoint tracking metrics of PID controller(mean±SD).

Phase	Rise time (min)	Overshoot (%)	Settling time (min)
1	2.57±0.61	0.02±0.26	1.96±0.69
2	6.62±3.92	-0.15±1.50	5.06±2.65
3	4.40±1.36	-0.29±0.60	3.43±1.12
Mean	4.53±1.96	0.15±0.79	3.48±1.49

TABLE 8. The evaluation of the PID controller performance.

Index	*MDPE*(%)	*MDAPE*(%)	*Wobble*(%)	*Divergence*(%)	IAE
mean±SD	0.20±0.01	0.20±0.01	0.19±0.01	-0.35±0.06	411±66

IV. DISCUSSION

In this study, we proposed a CLAD system based on the ACO-PID controller. RPE is first used as the DoH index in CLAD system for propofol anesthesia. The results showed that RPE has a higher P_k value than BIS in monitoring DoH. A virtual patient library is established based on a three-compartment PK model and PSO identification algorithm is employed for PD model's parameter optimization. The simulation results showed that the ACO optimization is feasible and effective in PID controller parameter optimization and that the anesthetic control manipulated by ACO-PID controller can track the DRPE curve quickly and accurately to meet the control requirement. The results also verified that different patients have different sensitivities to anesthetics.

RPE is a generalized form of permutation entropy, which is derived from symbolic dynamics and Renyi entropy. The permutation entropy measures the complexity of order pattern in the time series and has been widely used in physiological signal analysis [48], [49]. The central procedure of permutation entropy is the symbolic transform, which transforms the time-series recordings into a corresponding sequence of symbols by comparing the amplitude of the neighboring

time-series [32]. The merits of symbolic dynamics include: 1) insensitive to the amplitude of the time series, 2) more tolerance to noise, and 3) simple calculation [50]–[52]. The Renyi entropy is a generalized form of Shannon entropy, which can be adjusted by a parameter making it more sensitive to the events that occur seldomly or often [53]. Many studies have proven that the generalized entropy is prior to the Shannon entropy in EEG analysis [54], [55]. In our study, we further verified the effectiveness of RPE in estimating the DoH of propofol anesthesia and supported that the RPE has a potential in CLAD for propofol anesthesia.

To establish the virtual patient library, we utilized the PSO for parameter identification. Compared with other identification algorithms, the PSO algorithm is a population-based evolutionary algorithm, which is derived from artificial life and evolutionary computation theory. Furthermore, the PSO is simple and easy to implement, which does not have many parameters to adjust and does not need gradient information. PSO is also shown to be better in dealing with nonlinear continuous optimization problems, combinatorial optimization problems, and mixed-integer nonlinear optimization problems [56]. In this study, for the parameter identification of PD model, it is impossible to determine the specific range of initial parameters for identification because the parameters of these virtual patients are different. The PSO algorithm does not need too much prior knowledge of initialization values; it only needs a wide search range of initial parameters to obtain optimal identification. Therefore, we choose the PSO algorithm to solve the problem of parameter identification of PD model.

Because the initial parameters setting is an important issue in PID control, ACO is employed for optimal parameters search in our study. ACO algorithm is a population-based heuristic bionic evolutionary algorithm, compared with other optimization algorithms, such as genetic optimization algorithm, it is simpler, more robust and easier to parallelize [57], [58]. ACO algorithm is also shown to be efficiency since it does not depend on the exact mathematical model of the controlled object [59]. Thus, ACO algorithm can make the processing problem more flexible. Therefore, ACO algorithm is chosen to optimize parameters of PID controller, which can improve the quality of the system.

Most of the CLAD systems used BIS as the controlled variable, such as those in the studies of [2], [44]. In this study, we proposed a new DoH index for CLAD application. For a new DoH index, we needed to identify the related PD model parameters in the CLAD system. In the study of [2], and [44], the authors proposed improved PID controllers. We also employed the optimized PID (ACO-PID) and the results showed that ACO-PID is a comparable controller for propofol CLAD. Besides, the simulation results in this study can be compared with those in previous study, such as the results obtained by only using robust PID controller in [46]. The rise time and settling time in our study are smaller than those of [46], which indicates that the response of system is faster. Also, the overshoot in our study is (0.15 ± 0.79), which is much smaller than the studies of [46] and [8]. This means that the ACO-PID is more stable than the controller used in those studies. As we know, the PSO based PID control has also been used in mobile robots, aircraft, etc. [60], [61]. It was suggested that the PSO-PID has the advantages of good tracking performance. However, some other studies showed that PSO based PID is easy to fall into local extremum and slow convergence rate in the later stage of evolution [62], [63]. Also, from the perspective of clinical practice, whether the controller can work online is a particularly important merit. Therefore, further study is needed to improve CLAD and make it more convenient for users.

The ultimate aim of designing the CLAD system is for clinical application. However, the experiments require serious regulatory steps, and clinic practice involves many harsh restrictions. To make the simulation process close to real clinical practice, the control methods and validation procedures proposed in this study considered the actual rate of drug delivery in clinical practice. Moreover, information on the virtual patient model is obtained from clinical administration of actual patients. These simulations and optimizations based on virtual patients may provide useful knowledge for actual clinical experiments.

Despite this preliminary feasibility study showing that the ACO-PID controller and RPE controlled variable were suitable for propofol CLAD, there are still some limitations should be considered. First, in this study, we only simulated the closed-loop control based on the virtual patients, further validation is needed with practical clinical experiments. Second, the underlying assumption of the patient's model is that Schnider's model can perfectly describe the patient's effects individually, but this cannot actually be achieved in reality [44]. In order to achieve adequate control, individual identification is essential for the patient's model. Furthermore, some other popular PKPD models, such as Marsh's model, should also be considered in the future. Third, the measurement noise derived from the patient movement and surgical stimulation may influence the DoH index. The designed controller should be stable in the situation of the poor signal quality. In this study, we have considered the noise of surgical stimulation. The robust controller still needs to be enhanced to tolerate measurement noise.

V. CONCLUSION

In conclusion, our findings demonstrated the possibility of using RPE for DoH monitoring and ACO-PID for closed-loop control in propofol anesthesia. The RPE is a promising measurement for a robust nonlinear EEG analysis. The ACO-PID has potential application value for CLAD. In the further study, we will attempt to investigate whether the ACO-PID has potential in closed-loop control of inhalation anesthesia and combined anesthesia. We expect that PRE combined with ACO-PID can be applied to the practical CLAD and can serve as an important tool for accurate anesthetic administration.

APPENDIX

The appendix consists of five parts. The part A includes six figures. The part B is the description of PSO. The part C is the details of data set. The part D is the concrete optimization process of ACO. The part E is the introduction to P_k.

A. FIGURE PART

Fig. 8. demonstrates the parameters adjusting of PID based on the ACO. Fig. 9. is the results of anesthesia closed-loop simulation with a DRPE of 50, 40, 60 and 50. Fig. 10. shows the artificially generated stimulation disturbance signal. There are eight stages and each one represents a specific event during the surgery: 1) Stimulus A is the response to intubation; 2) Stimulus B represents a surgical incision followed by a time period with no stimulation; 3) Block C denotes an abrupt stimulus; 4) D represents the onset of a continuous normal stimulation during surgery; 5) The blocks of E, F, and G are the simulation of the surgical stimulation with short-lasting and strong strength; 6) Stage G simulates the scenario of the surgery during the closing period. Based on the simulated disturbance signal, the closed-loop anesthesia simulation of 12 patients are shown in Fig. 11.

B. DESCRIPTION OF PSO

The PSO algorithm can be summarized as follows:

Assume that the dimension of the search space is D. The position of i particle is $Y_i = (y_{i1}, y_{i2}, \ldots, y_{id})$. The speed of particle i is $V_i = (v_{i1}, v_{i2}, \cdots v_{id})$. And the dynamic range of the particles is $Y_{\max} = (y_{1\max}, y_{2\max}, \ldots, y_{d\max})$, which is the location of particle i. The maximum speed of each particle i is set to $V_{\max} = (v_{1\max}, v_{2\max}, \cdots v_{d\max})^T$. The individual extreme point is expressed by p_{id}, and the other global extremum is expressed by p_{gd}. The particle's speed and position are updated based on the following equations:

$$v_{id}^{h+1} = w \cdot v_{id}^{h} + C_1 \cdot rand_1 \cdot (p_{id} - x_{id}^{h}) + C_2 \cdot rand_2 \cdot (p_{gd} - x_{id}^{h}) \quad \text{(S1)}$$

$$y_{id}^{h+1} = y_{id}^{h} + v_{id}^{h+1} \quad \text{(S2)}$$

where C_1 and C_2 are the acceleration coefficients, which adjust the maximum step size of flying to the best particle and individual best particle. v_{id}^{h} represents the speed of the d_{th} dimension of particle i in the h_{th} iteration. x_{id}^{h} is the location of the d_{th} dimension of particle i in the h_{th} iteration. h is number of iterations. Where w is the inertia weight. Previous study showed that PSO can work effectively and stably in a noisy environment, and in many situations, the existence of noise can also help PSO avoid falling into local optimum. Eberhart et al proposed a dynamic inertia weight to try to solve this problem [65]. Therefore, inertia weight w is defined as follows:

$$w = 0.5 + \frac{rand(\cdot)}{2} \quad \text{(S3)}$$

where $rand(\cdot)$ is a uniformly distributed random number that is constrained within [0, 1]. In the study of reference [66], the initial inertia weight and acceleration coefficients were set to 0.729 and 1.494, respectively [65], [67]. We added a random disturbance on the inertia weight and acceleration coefficients. Therefore, the initial parameters of PSO are $w = 0.729 + random$ and $C_1 = C_2 = 1.494 + random$, where $random$ is a random number between [0, 1].

To prevent particles from moving away from the search space, the parameter v_d needs to be set in the range of $[-v_{d\max}, +v_{d\max}]$. We set the parameter range of $v_{d\max}$ to $[-2, +2]$ according to the study of [68], and the population is randomly generated. The position of the initial search point and its velocity were randomly generated within the allowable range. Parameters $rand_1$ and $rand_2$ were set as different random numbers between 0 and 1.

C. DETAILS OF DATA SET

To identify the model parameters of PD to achieve an accurate ERPE estimation in the control system, we examined two EEG data sets from twelve subjects. The first data set has eight human volunteers introduced in a previous study [38], who were only injected with propofol during the procedure. The propofol intravenous infusion of 150 ml/h (1500 mg/h) was administered to an antecubital vein through a syringe driver pump. All the subjects underwent the process from losing consciousness to recovering it. The raw EEG signals were recorded with the Aspect A-1000 EEG monitor with a sampling frequency of 128 Hz. The silver-silver chloride scalp electrodes were placed near the position of Fp1-F7.

The second EEG data set include eight patients undergoing outpatient elective colonoscopy procedure in the Anesthesia and operation central, Chinese PLA general hospital. The drug administration is similar to the first data set, only the propofol was used for sedation. All patients were ASA class I or II. The protocol and informed consent statements were approved by the Institutional Review Board at Chinese PLA general hospital. The raw EEG signals were recorded with BIS VISTA monitoring system with a sampling frequency of 128 Hz. The electrodes of second data set placed at the position near Fpz-F7 leads of 10-20 standard EEG montage.

D. SPECIFIC OPTIMIZATION PROCESS OF ACO

The specific optimization process of ACO is as follows: The integral absolute error Q is usually used as an evaluation of performance indicators in the project.

$$Q = \int_0^{\infty} t\,|e(t)\mathrm{d}t| \quad \text{(S4)}$$

Assuming that the total number of ants is m, for each ant i, the objective function value should be defined as follows:

$$\Delta Q_{ij} = Q_i - Q_j, \quad \forall i, j \quad \text{(S5)}$$

The transition probability of ant i at time t is defined as follows:

$$P_{ij}(t) = \begin{cases} \dfrac{[\tau_{ij}]^{\alpha}[\Delta Q_{ij}(t)]^{\beta}}{\sum\limits_{r \in allowed}[\tau_{ir}(t)]^{\alpha}[\Delta Q_{ir}]^{\beta}}, & j \in \text{allowed} \\ 0, & \text{other} \end{cases} \tag{S6}$$

where α is information heuristic factor, and β is expected heuristic factor, respectively.$\tau_{ij}(t)$ is the pheromone intensity between place i and place j at the current t time. $\Delta Q_{ij}(t)$ is the attractiveness of the path, describing the expected strength of preferential selection of the path.

When the ants went through a path, the pheromone intensity of the path was updated according to the following formula:

$$\tau_{ij}(t+k) = \rho\tau_{ij}(t) + \sum_{l=1}^{m} \Delta\tau_{ij}^{l} \tag{S7}$$

where ρ is the pheromone evaporation coefficient.

The $\Delta\tau_{ij}^{l}$ in equation (S7) denotes the residual pheromone and is defined as follows:

$$\Delta\tau_{ij}^{l} = \begin{cases} \frac{F}{Q_l}, \text{if ant } l \text{ passed the path } ij \text{during this cycle} \\ 0, \text{otherwise} \end{cases} \tag{S8}$$

where F is the pheromone intensity, and Q_l is the path length of ant l between i and j.

Ants will update according to pheromone update rules given by equation (S7) and (S8). Repeating the above process, the ant population finally found the optimal solution of the PID controller parameters.

E. INTRODUCTION TO P_k

In this study, to compare the performance of BIS and RPE in tracking the ESC of propofol, we calculated the prediction probability P_k [21]. Firstly, took the ESC and RPE(or BIS) value as $S(k)$ and $I(k)$, $k = 1, 2, \ldots, N$(N is the number of the indices during the time course), we chose two data points $S(i)$ and $S(j)(S(i) \neq S(j), i \neq j)$ randomly. Secondly, the monotony of $S(i)$ and $S(j)$ with the monotony of $I(i)$ and $I(j)$ was compared. When the monotony of $I(i)$ and $I(j)$ was same as the monotony of $S(i)$ and $S(j)$, we regarded the $I(i)$ and $I(j)$ as a concordance. And the $I(i)$ and $I(j)$ were x-only tie when $I(i)$ equaled to $I(j)$. Otherwise, the relationship of $I(i)$ and $I(j)$ was considered as a discordance. Thirdly, the above procedures were repeated for $5*N$ times (N is the number of the time points the indices measured during a time course). The P_k was defined as:

$$P_k = \frac{P_c + P_{tx}/2}{P_c + P_d + P_{tx}} \tag{S9}$$

where P_c, P_d, and P_{tx} were the respective proportions that $I(i)$ and $I(j)$ were a concordance, discordance, or an x-only tie. $P_k = 1$ of the RPE or BIS meant that the indices could correctly predict the ESC of propofol. A P_k value of 0.5 indicated that indicators (RPE or BIS) were no better than chance in predicting the ESC of propofol. Considering the decrease of RPE and BIS with the increase of propofol concentration, the P_k value was replaced by $1 - P_k$ in this study.

ACKNOWLEDGMENT

(Lingyun Fu and Xiaoyu Li contributed equally to this work.)

REFERENCES

[1] M. Fang, Y. Tao, and Y. Wang, "An enriched simulation environment for evaluation of closed-loop anesthesia," *J. Clin. Monit. Comput.*, vol. 28, no. 1, pp. 13–26, 2014.

[2] F. Padula, C. Ionescu, N. Latronico, M. Paltenghi, A. Visioli, G. Vivacqua, "Optimized PID control of depth of hypnosis in anesthesia," *Comput. Methods Programs Biomed.*, vol. 144, pp. 21–35, Jun. 2017.

[3] S. N. Ching and E. N. Brown, "Modeling the dynamical effects of anesthesia on brain circuits," *Current Opinion Neurobiol.*, vol. 25, no. 2, pp. 116–122, 2014.

[4] T. W. Schnider, C. F. Minto, P. L. Gambus, C. Andresen, D. B. Goodale, S. L. Shafer, and E. J. Youngs, "The influence of method of administration and covariates on the pharmacokinetics of propofol in adult volunteers," *Anesthesiology*, vol. 88, no. 5 , pp. 1170–1182, 1998.

[5] A. Gentilini, C. Schaniel, M. Morari, C. Bieniok, R. Wymann, and T. Schnider, "A new paradigm for the closed-loop intraoperative administration of analgesics in humans," *IEEE Trans. Biomed. Eng.*, vol. 49, no. 4, pp. 289–299, Apr. 2002.

[6] H. Schwilden, J. Schüttler, and H. Stoeckel, "Closed-loop feedback control of methohexital anesthesia by quantitative EEG analysis in humans," *Anesthesiology*, vol. 67, no. 3, pp. 341–347, 1987.

[7] N. Liu, M. Le Guen, F. Benabbes-Lambert, T. Chazot, B. Trillat, D. I. Sessler, and M. Fischler, "Feasibility of closed-loop titration of propofol and remifentanil guided by the spectral M-Entropy monitor," *Anesthesiology*, vol. 116, no. 2, pp. 286–295, 2012.

[8] J.-O. Hahn, G. A. Dumont, and J. M. Ansermino, "Robust closed-loop control of hypnosis with propofol using WAV_{CNS} index as the controlled variable," *Biomed. Signal Process. Control*, vol. 7, no. 5, pp. 517–524, 2012.

[9] M. M. R. F. Struys, T. De Smet, S. Greenwald, A. R. Absalom, S. Bingé, and E. P. Mortier, "Performance evaluation of two published closed-loop control systems using bispectral index monitoring: A simulation study," *Anesthesiology*, vol. 100, no. 3, pp. 640–647, 2004.

[10] S. Bibian, G. A. Dumont, and T. Zikov, "Dynamic behavior of BIS, M-entropy and neuroSENSE brain function monitors," *J. Clin. Monit. Comput.*, vol. 25, no. 1, pp. 81–87, 2011.

[11] J. C. Henry, *Electroencephalography: Basic Principles, Clinical Applications, and Related Fields*. Munich, Germany: Urban & Schwarzenberg, 1982, p. 654.

[12] Z. Liang, D. Li, G. Ouyang, Y. Wang, L. J. Voss, J. W. Sleigh, and X. Li, "Multiscale rescaled range analysis of EEG recordings in sevoflurane anesthesia," *Clin. Neurophysiol.*, vol. 123, no. 4, pp. 681–688, 2012.

[13] A. Shalbaf, M. Saffar, J. W. Sleigh, and R. Shalbaf, "Monitoring the depth of anesthesia using a new adaptive neurofuzzy system," *IEEE J. Biomed. Health Inform.*, vol. 22, no. 3, pp. 671–677, May 2018.

[14] P. Gifani, H. R. Rabiee, M. H. Hashemi, P. Taslimi, and M. Ghanbari, "Optimal fractal-scaling analysis of human EEG dynamic for depth of anesthesia quantification," *J. Franklin Inst.*, vol. 344, nos. 3–4, pp. 212–229, 2007.

[15] J. Alvarez-Ramirez, J. C. Echeverria, and E. Rodriguez, "Performance of a high-dimensional R/S method for Hurst exponent estimation," *Phys. A, Stat. Mech. Appl.*, vol. 387, no. 26, pp. 6452–6462, 2008.

[16] T. Nguyen-Ky, P. Wen, and Y. Li, "Improving the accuracy of depth of anaesthesia using modified detrended fluctuation analysis method," *Biomed. Signal Process. Control*, vol. 5, no. 1, pp. 59–65, 2010.

[17] J. Fell, J. Röschke, K. Mann, and C. Schäffner, "Discrimination of sleep stages: A comparison between spectral and nonlinear EEG measures," *Electroencephalogr. Clin. Neurophysiol.*, vol. 98, no. 5, pp. 401–410, 1996.

[18] X. Li, S. Cui, and L. J. Voss, "Using permutation entropy to measure the electroencephalographic effects of sevoflurane," *Anesthesiology*, vol. 109, no. 3, p. 448–456, 2008.

[19] L. A. Manilo and S. S. Volkova, "Recognition of the deep anesthesia stage from parameters of the approximated entropy of EEG signal," *Pattern Recognit. Image Anal.*, vol. 23, no. 1, pp. 92–97, Jun. 2013.

[20] Z. Liang, Y. Wang, X. Sun, D. Li, L. J. Voss, J. W. Sleigh, S. Hagihira, and X. Li, "EEG entropy measures in anesthesia," *Frontiers Comput. Neurosci.*, vol. 9, p. 16, Feb. 2015.
[21] Z. Liang, Y. Ren, J. Yan, D. Li, L. J. Voss, J. W. Sleigh, and X. Li, "A comparison of different synchronization measures in electroencephalogram during propofol anesthesia," *J. Clin. Monit. Comput.*, vol. 30, no. 4, pp. 451–466, 2016.
[22] B. Marsh, M. White, N. Morton, And G. N. C. Kenny, "Pharmacokinetic model driven infusion of propofol in children," *Brit. J. Anaesthesia*, vol. 67, no. 1, pp. 41–48, 1991.
[23] I. Martín-Mateos, J. A. M. Pérez, J. A. R. Morales, and J. F. Gómez-González, "Adaptive pharmacokinetic and pharmacodynamic modelling to predict propofol effect using BIS-guided anesthesia," *Comput. Biol. Med.*, vol. 75, pp. 173–180, Apr. 2016.
[24] J. Schüttler and H. Ihmsen, "Population pharmacokinetics of propofol: A multicenter study," *Anesthesiology*, vol. 92, no. 3, pp. 727–738, 2000.
[25] G. D. Puri, "Target controlled infusion total intravenous anaesthesia and Indian patients: Do we need our own data?" *Indian J. Anaesthesia*, vol. 62, no. 4, pp. 245–248, 2018.
[26] J. Kennedy and R. C. Eberhart, "Particle swarm optimization," in *Proc. IEEE Int. Conf. Neural Netw.*, vol. 4, Nov. 1995, pp. 1942–1948.
[27] C. M. Ionescu, I. Nascu, and R. De Keyser, "Robustness tests of a model based predictive control strategy for depth of anesthesia regulation in a propofol to bispectral index framework," in *Proc. Int. Conf. Advancements Med. Health Care Through Technol.* Springer, 2011, pp. 234–239.
[28] K. van Heusden, K. Soltesz, E. Cooke, S. Brodie, N. West, M. Gorges, J. M. Ansermino, and G. Dumont, "Optimizing robust PID control of propofol anesthesia for children; Design and clinical evaluation," *IEEE Trans. Biomed. Eng.*, to be published.
[29] D. Sandoval, I. Soto, and P. Adasme, "Control of direct current motor using Ant Colony optimization," in *Proc. CHILEAN Conf. Elect., Electron. Eng., Inf. Commun. Technol.*, Oct. 2016, pp. 79–82.
[30] F. A. G. S. Babu and B. T. Chiranjeevi, "Implementation of fractional order PID controller for an AVR system using GA and ACO optimization techniques," *IFAC PapersOnLine*, vol. 49, no. 1, pp. 456–461, 2016.
[31] M. Aabid, A. Elakkary, and N. Sefiani, "PID parameters optimization using ant-colony algorithm for human heart control," in *Proc. 23rd Int. Conf. Automat. Comput.*, Sep. 2017, pp. 1–6.
[32] C. Bandt and B. Pompe, "Permutation entropy: A natural complexity measure for time series," *Phys. Rev. Lett.*, vol. 88, no. 17, 2002, Art. no. 174102.
[33] Z. Wang, J. Li, K. Fan, W. Ma, and H. Lei, "Prediction method for low speed characteristics of compressor based on modified similarity theory with genetic algorithm," *IEEE Access*, vol. 6, pp. 36834–36839, 2018.
[34] M. E. C. Bento, D. Dotta, R. Kuiava, and R. A. Ramos, "A procedure to design fault-tolerant wide-area damping controllers," *IEEE Access*, vol. 6, pp. 23383–23405, 2018.
[35] W.-H. Ho, J.-T. Tsai, J.-H. Chou, and J.-B. Yue, "Intelligent hybrid Taguchi-genetic algorithm for multi-criteria optimization of shaft alignment in marine vessels," *IEEE Access*, vol. 4, pp. 2304–2313, 2017.
[36] N. Hou, F. He, Y. Zhou, Y. Chen, and X. Yan, "A parallel genetic algorithm with dispersion correction for HW/SW partitioning on multi-core CPU and many-core GPU," *IEEE Access*, vol. 6, pp. 883–898, 2017.
[37] D. N. Le, "PSO and ACO algorithms applied to optimization resource allocation to support QoS requirements in NGN," *Int. J. Inf. Netw. Secur.*, vol. 2, no. 3, pp. 216–228, 2013.
[38] M. L. Williams and J. W. Sleigh, "Auditory recall and response to command during recovery from propofol anaesthesia," *Anaesthesia Intensive Care*, vol. 27, no. 3, pp. 265–268, 1999.
[39] M. M. Mukaka, "Statistics corner: A guide to appropriate use of Correlation coefficient in medical research," *Malawi Med. J.*, vol. 24, no. 3, pp. 69–71, 2012.
[40] J. R. Varvel, D. L. Donoho, and S. L. Shafer, "Measuring the predictive performance of computer-controlled infusion pumps," *J. Pharmacokinetics Biopharmaceutics*, vol. 20, no. 1, pp. 63–94, 1992.
[41] I. Naşcu, R. Oberdieck, and E. N. Pistikopoulos, "Explicit hybrid model predictive control strategies for intravenous anaesthesia," *Comput. Chem. Eng.*, vol. 106, pp. 814–825, Nov. 2017.
[42] J. D. Laycock, "Signs and stages of anæsthesia a restatement," *Anaesthesia*, vol. 8, no. 1, pp. 15–20, 1953.
[43] A. E. Guedel, "Stages of anesthesia and a re-classification of the signs of anesthesia," *Anesthesia Analgesia*, vol. 6, no. 4, pp. 157–162, 1927.
[44] K. Soltesz, J.-O. Hahn, T. Hägglund, G. A. Dumont, and J. M. Ansermino, "Individualized closed-loop control of propofol anesthesia: A preliminary study," *Biomed. Signal Process. Control*, vol. 8, no. 6, pp. 500–508, 2013.
[45] M. Araki and E. Furutani, "Computer control of physiological states of patients under and after surgical operation," *Annu. Rev. Control*, vol. 29, no. 2, pp. 229–236, 2005.
[46] G. A. Dumont, A. Martinez, and J. M. Ansermino, "Robust control of depth of anesthesia," *Int. J. Adapt. Control Signal Process.*, vol. 23, no. 5, pp. 435–454, 2008.
[47] S. Yelneedi, L. Samavedham, and G. P. Rangaiah, "Advanced control strategies for the regulation of hypnosis with propofol," *Ind. Eng. Chem. Res.*, vol. 48, no. 8, pp. 3880–3897, 2009.
[48] R. Edwards, H. T. Siegelmann, K. Aziza, and L. Glass, "Symbolic dynamics and computation in model gene networks," *Chaos, Interdiscipl. J. Nonlinear Sci.*, vol. 11, no. 1, pp. 160–169, 2001.
[49] F. Biessmann, S. Plis, F. C. Meinecke, T. Eichele, and K.-R. Muller, "Analysis of multimodal neuroimaging data," *IEEE Rev. Biomed. Eng.*, vol. 4, pp. 26–58, 2012.
[50] D. Abásolo, R. Hornero, C. Gómez, M. García, and M. López, "Analysis of EEG background activity in Alzheimer's disease patients with Lempel–Ziv complexity and central tendency measure," *Med. Eng. Phys.*, vol. 28, no. 4, pp. 315–322, 2006.
[51] R. Ferenets, T. Lipping, A. Anier, V. Jantti, S. Melto, and S. Hovilehto, "Comparison of entropy and complexity measures for the assessment of depth of sedation," *IEEE Trans. Biomed. Eng.*, vol. 53, no. 6, pp. 1067–1077, Jun. 2006.
[52] Z. Liang, S. Liang, Y. Wang, G. Ouyang, and X. Li, "Tracking the coupling of two electroencephalogram series in the isoflurane and remifentanil anesthesia," *Clin. Neurophysiol.*, vol. 126, no. 2, pp. 412–422, 2015.
[53] L. Zunino, D. G. Pérez, A. Kowalski, M. T. Martín, M. Garavaglia, A. Plastino, and O. A. Rosso, "Fractional Brownian motion, fractional Gaussian noise, and Tsallis permutation entropy," *Phys. A, Stat. Mech. Appl.*, vol. 387, no. 24, pp. 6057–6068, 2008.
[54] J. Lerga, J. Lerga, and V. Mozetič, "Algorithm based on the short-term RÃlnyi entropy and IF estimation for noisy EEG signals analysis," *Comput. Biol. Med.*, vol. 80, pp. 1–13, Jan. 2017.
[55] Y. Tonoyan, T. Chanwimalueang, D. P. Mandic, and M. M. Van Hulle, "Discrimination of emotional states from scalp-and intracranial EEG using multiscale Rényi entropy," *PLoS One*, vol. 12, no. 11, 2017, Art. no. e0186916.
[56] G. C. Chen and Y. U. Jin-Shou, "Particle swarm optimization algorithm," *Inf. Control*, vol. 186, no. 3, pp. 454–458, 2005.
[57] J. Montgomery and M. Randall, "Anti-pheromone as a tool for better exploration of search space," in *Proc. Int. Workshop Ant Algorithms*, 2002, pp. 100–110.
[58] A. S. Oshaba, E. S. Ali, and S. M. A. Elazim, "ACO based speed control of SRM fed by photovoltaic system," *Int. J. Electr. Power Energy Syst.*, vol. 67, pp. 529–536, May 2015.
[59] M. Tuba and R. Jovanovic, "Improved aco algorithm with pheromone correction strategy for the traveling salesman problem," *Int. J. Comput. Commun.*, vol. 8, no. 3, pp. 477–485, Apr. 2013.
[60] L.-C. Lai, Y.-C. Chang, J.-T. Jeng, G.-M. Huang, W.-N. Li, and Y.-S. Zhang, "A PSO method for optimal design of PID controller in motion planning of a mobile robot," in *Proc. Int. Conf. Fuzzy Theory Appl.*, Dec. 2014, pp. 134–139.
[61] P. Biswas, R. Maiti, A. Kolay, K. D. Sharma, and G. Sarkar, "PSO based PID controller design for twin rotor MIMO system," in *Proc. Int. Conf. Control, Instrum., Energy Commun. (CIEC)*, Jan./Feb. 2014, pp. 56–60.
[62] K. Ishaque, Z. Salam, M. Amjad, and S. Mekhilef, "An improved particle swarm optimization (PSO)–based MPPT for PV with reduced steady-state oscillation," *IEEE Trans. Power Electron.*, vol. 27, no. 8, pp. 3627–3638, Aug. 2012.
[63] X. Liu, D. Zhao, and Y. Wu, "Application of improved PSO in PID parameter optimization of quadrotor," in *Proc. Int. Comput. Conf. Wavelet Active Media Technol. Inf. Process.*, Dec. 2016, pp. 443–447.
[64] R. A. Hanifah, S. F. Toha, and S. Ahmad, "PID-Ant colony optimization (ACO) control for electric power assist steering system for electric vehicle," in *Proc. IEEE Int. Conf. Smart Instrum., Meas. Appl. (ICSIMA)*, Nov. 2013, pp. 1–5.
[65] R. C. Eberhart and Y. Shi, "Particle swarm optimization: Developments, applications and resources," in *Proc. Congr. Evol. Comput.*, May 2002, pp. 81–86.

[66] A. Ratnaweera, S. K. Halgamuge, and H. C. Watson, "Self-organizing hierarchical particle swarm optimizer with time-varying acceleration coefficients," *IEEE Trans. Evol. Comput.*, vol. 8, no. 3, pp. 240–255, Jun. 2004.
[67] M. Clerc and J. Kennedy, "The particle swarm—Explosion, stability, and convergence in a multidimensional complex space," *IEEE Trans. Evol. Comput.*, vol. 6, no. 1, pp. 58–73, Feb. 2002.
[68] Y. Shi and R. C. Eberhart, *Parameter Selection in Particle Swarm Optimization*. Berlin, Germany: Springer, 1998, pp. 591–600.

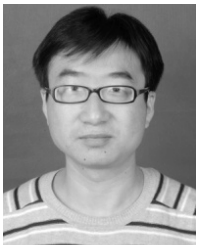

ZHENHU LIANG received the B.Eng. degree in mechanical engineering and the Ph.D. degree in automation from Yanshan University, China, in 2004 and 2012, respectively, where he is currently an Associate Professor with the Department of Automation. His current research interests include neural engineering, signal processing, data analysis, and monitoring system design.

LINGYUN FU received the B.S. degree in automation from Yanshan University, Qinhuangdao, China, in 2017, where she is currently pursuing the master's degree with the Department of Automation. Her research interests include the closed-loop control of anesthesia and machine learning.

XIAOYU LI received the B.S. and M.A. degrees in automation from Yanshan University, Qinhuangdao, China, in 2015 and 2018, respectively. Her research interest includes the closed-loop control of anesthesia at different age stages.

ZEGUO FENG is currently an Associate Professor and the Chief Physician of Anesthesiology, Chinese PLA General Hospital. He is also the Deputy Director of the Anesthesia Operation Center, a Tutor of master's degree students with the Chinese PLA General Hospital, and the Deputy Head of the Orthopedic Anesthesiology Group, Chinese Medical Association. He is good at complex liver surgery, the resection of giant retroperitoneal tumors, anesthesia for elderly critically ill patients, perioperative volume therapy, and monitoring management research.

JAMIE W. SLEIGH is currently a Professor of anesthesiology and intensive care with the Waikato Clinical School, Waikato Hospital, and The University of Auckland, Hamilton, New Zealand. He grew up in Zimbabwe and specialized in anesthesia in the U.K., before moving to New Zealand, in 1988. He has practiced in both intensive care medicine and anesthesia—with particular interests in anesthesia for vascular surgery and neurosurgery. His current research interests include the practical use of EEG in anesthesia, EEG signal processing, the modeling of brain dynamics in anesthesia, sleep, and seizures, the pharmacokinetics of anesthetic drugs, and the molecular determinants of postoperative pain.

HAK KEUNG LAM received the B.Eng. (Hons.) and Ph.D. degrees from the Department of Electronic and Information Engineering, The Hong Kong Polytechnic University, Hong Kong, in 1995 and 2000, respectively. From 2000 to 2005, he was with the Department of Electronic and Information Engineering, The Hong Kong Polytechnic University, as a Postdoctoral Fellow and a Research Fellow. He joined King's College London, in 2005, as a Lecturer, where he is currently a Reader. He has coauthored a monograph such as *Stability Analysis of Fuzzy-Model-Based Control Systems* (Springer, 2011). His current research interests include intelligent control systems and computational intelligence. He has served as a program committee member and an international advisory board member for various international conferences. He is the coeditor of two edited volumes, including *Control of Chaotic Nonlinear Circuits* (World Scientific, 2009) and *Computational Intelligence and Its Applications* (World Scientific, 2012). He is an Associate Editor of the IEEE TRANSACTIONS ON FUZZY SYSTEMS, *IET Control Theory and Applications*, and the *International Journal of Fuzzy Systems and Neurocomputing*, and a Guest Editor of a number of international journals. He was also a reviewer for various books, international journals, and international conferences.